Identification of Reactive Species in Photoexcited Nanocrystalline TiO_2 Films by Wide-Wavelength-Range (400−2500 nm) Transient Absorption Spectroscopy

Toshitada Yoshihara,[†,‡] Ryuzi Katoh,*[,†,‡] Akihiro Furube,[†,‡] Yoshiaki Tamaki,[†,‡,§] Miki Murai,[†,‡] Kohjiro Hara,[†,‡] Shigeo Murata,[†,‡] Hironori Arakawa,[†,‡] and M. Tachiya[‡]

Photoreaction Control Research Center (PCRC) and National Institute of Advanced Industrial Science and Technology (AIST), Tsukuba Central 5, 1-1-1 Higashi, Tsukuba, Ibaraki 305-8565, Japan

Received: December 11, 2003

Reactive species, holes, and electrons in photoexcited nanocrystalline TiO_2 films were studied by transient absorption spectroscopy in the wavelength range from 400 to 2500 nm. The electron spectrum was obtained through a hole-scavenging reaction under steady-state light irradiation. The spectrum can be analyzed by a superposition of the free-electron and trapped-electron spectra. By subtracting the electron spectrum from the transient absorption spectrum, the spectrum of trapped holes was obtained. As a result, three reactive species—trapped holes and free and trapped electrons—were identified in the transient absorption spectrum. The reactivity of these species was evaluated through transient absorption spectroscopy in the presence of hole- and electron-scavenger molecules. The spectra indicate that trapped holes and electrons are localized at the surface of the particles and free electrons are distributed in the bulk.

Introduction

Photocatalytic reactions using TiO_2 have been attracting much interest because they can be applied to water splitting,[1] the degradation of environmental pollutants,[2,3] air purification,[2,3] solar energy conversion,[4,5] and so on. A lot of fundamental research has been carried out, and results from some of these studies have been successfully applied in industry. The primary reaction process is photoinduced electron transfer at the TiO_2 surface, which suggests that a large surface area is required for a highly efficient reaction. Thus, ultrafine particles have been widely used for practical applications.[2,3,6,7] Surface properties are important for achieving high photocatalytic activities, and there have been many attempts to modify the surface.[6−12]

Ultrafine TiO_2 particles are useful and relatively easy to prepare. Because photocatalytic reactions are usually examined in solution, the ultrafine particles in slurries must be separated from the products after the reactions. Separation can be a crucial problem, especially in industrial applications. Recently, nanocrystalline semiconductor films were developed. They are prepared by the calcination of primary ultrafine particles so that the films have large surface areas, and they maintain the high reactivity of the particles. Such a film shape is useful for handling in applications. These nanocrystalline films can be used as transparent electrodes, and their use as catalysts has also been studied.[13−15] In addition, the films are used as electrodes for dye-sensitized solar cells in which the films are covered with sensitizer dyes.[4,5]

The dynamics of photocatalytic reactions on TiO_2 particles have been studied extensively with the goal of determining the reaction mechanisms and thus improving photocatalytic reactivity.[16−60] Experimental techniques using pulsed lasers are useful for probing the behavior of photogenerated electrons and holes. Transient absorption spectroscopy in the femtosecond to millisecond time range has been used to study the generation, relaxation, and recombination processes of electrons and holes.[27−56] The presence of additional reactants in the solution makes it possible to probe the interfacial electron-transfer processes through this technique.[27−35,39−44,47,49]

For absorption spectroscopy, transparent samples are generally required. Therefore, colloidal nanoparticles have been investigated in many cases. However, the conditions surrounding the particles cannot be freely changed to prevent the aggregation and precipitation of the nanoparticles. Film samples are useful for preparing various experimental conditions.

In general, to probe chemical reactions by absorption spectroscopy, it is necessary to identify the absorption bands of the reactive species. However, for TiO_2 particles, a precise assignment of the absorptions of electrons and holes is rather difficult because their absorption spectra are very broad[16−22,24−35,38,39,41−43,46−50] and the bands overlap each other in the visible wavelength region. Moreover, the spectra are very sensitive to the characteristics of the TiO_2 particles, such as the crystal phase, particle size,[20,22,38,46,48] and surface conditions, even with otherwise identical samples. This problem complicates comparisons between the obtained spectra. In addition, electrons and holes seem to be distributed in various kinds of trapping sites in which they exhibit different absorption spectra and reactivity. Therefore, transient absorption spectra frequently show complicated temporal changes. This complexity has limited our understanding of the reaction mechanism despite many previous efforts to make transient absorption measurements.

Recently, transient absorption studies in the IR wavelength range were carried out to solve the above-mentioned problems.[51−60] In the IR wavelength range, the strong absorption due to conducting electrons is distinct, and its shape can be analyzed by means of a simple theoretical model based on solid-state physics. Therefore, spectral assignments are more reliable than in the visible region, and reaction kinetics can be precisely

* Corresponding author. E-mail: r-katoh@aist.go.jp.
† PCRC.
‡ AIST.
§ NEDO Fellow.

10.1021/jp031305d CCC: $27.50
Published on Web 02/28/2004

probed by means of temporal changes in the conducting-electron signal. Using microsecond transient IR spectroscopy, Yamakata et al. investigated the kinetics of conducting electrons in the reaction of TiO_2 particles with oxygen and water molecules.[53] Hoffmann et al. also reported a similar absorption of conducting electrons.[57−59] The vibrational bands of reactants also provide useful information about reaction processes.[51,54,56−60] However, one disadvantage of this technique is the difficulty in carrying out experiments on TiO_2 particles in media that strongly absorb in the IR region, such as water and organic solvents. In practice, most photocatalysis reactions occur under such conditions.

Because of this limitation and because IR spectroscopy cannot be used to monitor hole dynamics, species such as holes and surface-trapped electrons must be assigned by means of other methods. The development of such methods would be very useful for future investigations of various kinds of photocatalytic reactions of TiO_2 particles.

We thought that it might be possible to make assignments by simultaneously observing the transient absorption band appearing in the visible range and the band for the conducting electrons in the IR range. We measured the transient absorption spectra of TiO_2 nanocrystalline films over a wide spectral range from 400 to 2500 nm with a high degree of accuracy ($\sim 10^{-4}$ optical density (OD)). The absorption bands of trapped holes and free and trapped electrons were clearly identified in the spectra and were compared with literature spectra. We also studied some typical reactions of these species with scavenger molecules such as methanol and oxygen. These results confirmed that trapped holes and electrons are localized at the surface of particles and free electrons are in the bulk.

Experimental Section

TiO_2 nanoparticles were prepared by the method reported by Grätzel and co-workers.[61] The mean diameter of the primary nanoparticles was 10−15 nm. The organic paste containing the semiconductor nanoparticles was printed on a glass substrate by a screen-printing technique.[62] When the sample was calcined, the opaque film became transparent enough for spectroscopic measurements. The mean diameter increased slightly to about 20 nm, as measured by scanning electron microscopy. The crystal phase was anatase. The TiO_2 films were 1 cm^2 (1 cm × 1 cm) in area and 2−5 μm thick.

The nanocrystalline TiO_2 films were placed in several solutions for steady-state and time-resolved spectroscopic experiments. Heavy water (D_2O, Cambridge Isotope Laboratories, Inc., 99.8%) and methanol-d_4 (CD_3OD, Cambridge Isotope Laboratories, Inc., 99.8%) were used without further purification.

For transient absorption measurements, the third harmonic (355 nm) of a Nd^{3+}:YAG laser (HOYA Continuum, Surelite II) was employed for excitation. A Xe lamp (Hamamatsu, 150 W) and a halogen lamp (100 W) were used as probe light sources for the 400−800 and 800−2500 nm wavelength ranges, respectively. The probe light was introduced into a monochromator (ACTON, Spectra Pro-150) after passing through the sample specimen. The intensity of the probe light was detected by a Si photodiode (Hamamatsu, S-1722-02) in the 400−1000 nm range and a mercury cadmium telluride (MCT) photodetector (Dorotek, PDI-2TE-4) in the 900−2500 nm range. The photocurrent from the detectors was processed with an AC-coupled preamplifier (NF Electronic Instruments, SA-230F5) to extract only the transient signals, and the signals were magnified by an amplifier (NF Electronic Instruments, 5305). The amplified transient signals were recorded with a digital oscilloscope (Tektronix, TDS380C) and transferred to a personal computer for analysis. The DC offset of the photocurrent from the detector was subtracted using the preamplifier, and thus we could measure small absorbance changes ($<10^{-5}$). The time resolution of the overall system was about 50 ns. To calculate the absorbance change, we needed to know the intensity of the probe light without laser excitation, and it was measured by modulating the probe light intensity with an optical chopper placed in front of the detector. The intensity of the laser pulse was measured with a pyroelectric energy meter (Gentec, ED-200L). All measurements were carried out at 295 K.

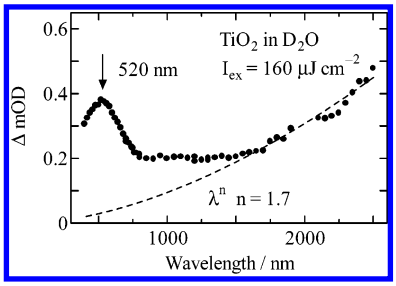

Figure 1. Transient absorption spectrum of a nanocrystalline TiO_2 film in N_2-saturated D_2O (●). The dashed line represents the theoretical curve λ^n, where $n = 1.7$.

For steady-state photoreaction measurements, a collimated UV light beam (270−390 nm) from a Xe lamp (Hamamatsu, 150 W) was used as an excitation light source. The light beam passed through a U340 filter (HOYA Optics Corporation) prior to the illumination of the nanocrystalline TiO_2 film in CD_3OD. The solution was deaerated by bubbling nitrogen through it for 30 min. The absorption change induced by UV light irradiation was measured with a UV−vis/near-IR spectrophotometer (Shimadzu, UV-3101PC).

Results and Discussion

Identification of Hole and Electron Absorptions in the Transient Absorption Spectrum of Nanocrystalline TiO_2 Films. Figure 1 shows the transient absorption spectrum of nanocrystalline TiO_2 films in N_2-saturated heavy water 1 μs after excitation. The intensity of the excitation light was 160 μJ cm^{-2}. Upon band-gap excitation, holes and electrons were produced, and their absorptions overlapped with each other in the broad absorption range. The absorption spectra of these species were very sensitive to their environment; that is, the peak positions and shapes reflected the trap depth. Under this condition, no quenching of the photogenerated carriers was expected, meaning that each TiO_2 particle had the same number of holes and electrons. The spectrum in the shorter-wavelength range (<1000 nm) is broad and shows a peak at 520 nm. In the near-IR wavelength range (1000−2500 nm), the absorbance increases with increasing wavelength (λ).

Figure 2 shows the decay profiles of the transient absorptions observed at 440, 550, 800, and 2300 nm. The intensity of the excitation light was 160 μJ cm^{-2}. All of the decay profiles are identical within experimental error; that is, the spectrum did not change before 1 μs. This result indicates that simple electron−hole recombination was observed without quenching with some impurities and that the trap distribution of the carriers in the particles did not change in the observed time period. These facts suggest that the relaxation and trapping of photogenerated electrons and holes occurred early and that all species were in thermal equilibrium.

To examine electron−hole recombination dynamics, we measured the decay profiles of the transient absorption at 600

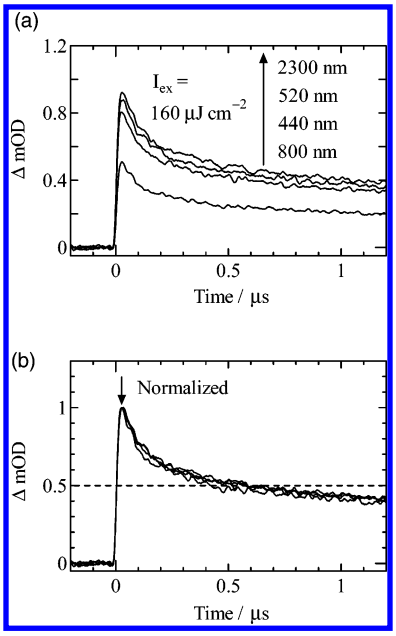

Figure 2. (a) Temporal profiles of transient absorption observed at 440, 520, 800, and 2300 nm. (b) Normalized profiles at time zero.

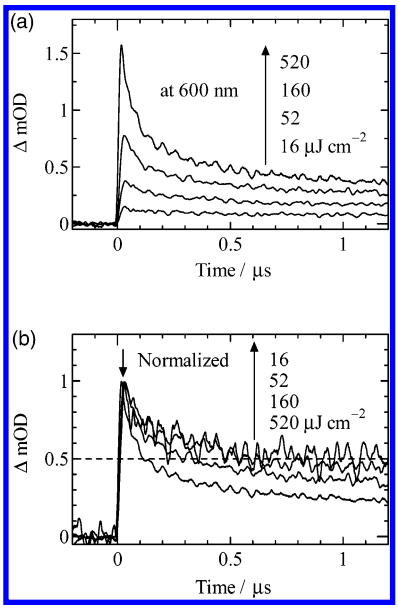

Figure 3. (a) Temporal profiles of transient absorption observed at 600 nm at $I_{ex} = 16$, 52, 160, and 520 μJ cm^{-2}. (b) Normalized profiles at time zero.

nm as a function of excitation light intensity (Figure 3). The fact that the decay rate seemed to increase with increasing excitation intensity suggests that bulk recombination between holes and electrons dominated the decay. At weak excitation intensities, by contrast, the decay profiles were similar to each other, which indicates that geminate recombination occurred. This result is consistent with the fact that the interparticle transfer of holes and electrons is expected to be slow. In fact, the estimated absorbed photon number per particle is less than unity at the weak excitation intensities. The decay profile under weak excitation conditions shows geminate recombination. Thus, the same kinetics can be expected under conditions of extremely weak light irradiation, such as sunlight irradiation.

As shown in Figure 3, the time profiles of the recombination are strongly affected by the light intensity. For a dye-sensitized nanocrystalline TiO_2 film, the recombination of injected electrons and parent cations has been studied by changing the light

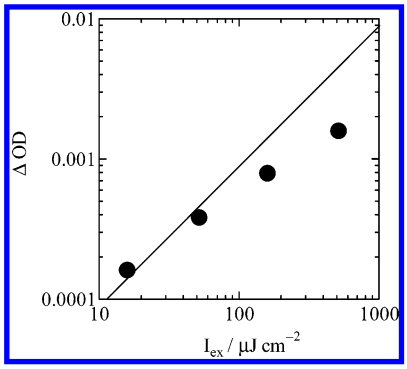

Figure 4. Absorbance change at time zero probed at 600 nm as a function of I_{ex}.

intensity and electrochemical bias.[63] An interpretation of these observations indicates that the increased recombination rate at higher excitation intensity is due to a trap-filling effect. The injected electrons are trapped immediately, and they occupy deep traps in the particles. Therefore, the effective mobility of other electrons increases. For bare TiO_2 films, a similar light-intensity dependence is observed (Figure 3), suggesting that the trap-filling model is applicable to bare TiO_2 films. Under weak excitation conditions, by contrast, there are many unoccupied deep traps; therefore, slow recombination is observed (Figure 3). The time profile cannot be fit by a single-exponential decay function. The nonexponential decay profile of recombination can be explained by using the model of recombination kinetics based on detrapping from deep traps.[64] Namely, the recombination rate is limited by the motion of electrons. Recently, Durrant and co-workers reported that the recombination kinetics in a dye-sensitized film becomes single exponential when a positive charge on a dye cation separates from the surface.[65] This indicates that single-exponential kinetics is realized when electron transfer between an electron and a positive charge is slower than the motion of charge carriers. The nonexponential decay profile in bare TiO_2 films (Figure 3) clearly shows that the rate of recombination is limited by the motion of electrons and holes in the particles.

There is a large difference in the decay rate between bare TiO_2 films and a dye-sensitized films. The recombination time has been evaluated as the time required for 50% of the initial absorbance ($t_{1/2}$) and has been found to be about 1 ms.[63] In our case, $t_{1/2}$ was about 1 μs, which is 3 orders of magnitude smaller than that of the dye-sensitized system. At present, the reason is unclear. As we discussed above, the rate of recombination in this system is limited by the effective mobility of charge carriers. Therefore, the differences in driving force and reorganization energy on the electron-transfer reaction are not the reason for the large difference in the recombination rate. For dye-sensitized films, parent cations are fixed on the surface of the particles, and for bare TiO_2 films, as we will discuss later, holes are trapped at the surface. Therefore, the locations of positive charge are similar to each other. Thus, the difference in the recombination rate between dye-sensitized films and bare films may be due to the difference in the effective mobility of the positive charge; that is, dye cations are fixed on the surface, but holes can migrate. This motion of holes is the rate-limiting process for electron−hole recombination in bare TiO_2 films.

Figure 4 shows the initial absorbance of each decay signal shown in Figure 3 as a function of excitation intensity, I_{ex}. At low excitation intensities, the initial absorbance seems to be proportional to the intensity, whereas at higher intensities, deviation from the straight line can be seen. This result indicates that bulk recombination is faster at higher intensities and,

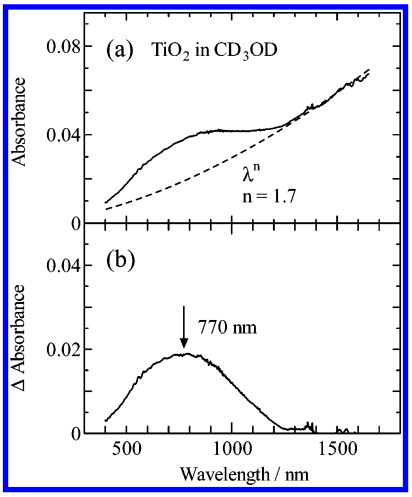

Figure 5. (a) Absorption spectrum of a TiO_2 film in N_2-saturated CD_3OD after irradiation with UV light for 30 min. The dashed line represents the theoretical curve λ^n, where $n = 1.7$. (b) Subtraction spectrum.

therefore, that the rapid decay of the signal cannot be detected within the time resolution of the measurement system (50 ns). We are investigating these dynamics using femtosecond transient absorption experiments, and the results will be published elsewhere.[66]

Here we analyze the shape of the transient absorption spectrum shown in Figure 1. In the near-IR wavelength range (1000−2500 nm), the absorbance increased with wavelength (λ). This pattern is characteristic of free electrons, and thus this absorbance can be assigned to the transition from the bottom of the conduction band to the upper levels in the same band (intraband transition).[67] Other groups have observed these structureless spectra in the infrared wavelength range for TiO_2 particles.[52,53,58] We have also observed a similar spectrum in nanocrystalline ZnO films.[68,69] According to a theoretical model for the intraband transition,[67] the absorbance A is proportional to λ^n. The spectrum shown in Figure 1 can be fit using $n = 1.7$ (the dashed line in Figure 1). This n value is similar to those reported for the longer-wavelength range (2200−10 000 nm).[52,53,58] In the IR wavelength range, we observed only electron absorption, which was confirmed by a hole-scavenging study.[54−56] Thus, we can assign the observed spectrum in the region higher than 1500 nm to the absorption of free electrons in TiO_2 particles. By extrapolating the spectral shape of free electrons toward the visible range on the basis of a theoretical model, we were able to assign the absorption bands of the free electrons in the whole spectral range examined. By using this spectrum, we were then able to determine the absorption bands of other species.

By quenching the holes, we were able to deal with only electrons. Figure 5a shows the absorption spectrum of a nanocrystalline TiO_2 film in CD_3OD after irradiation with UV light (270−390 nm) for 30 min under bubbling N_2. This technique is commonly used to detect electrons in nanoparticle suspensions.[16−18] Under these conditions, holes react with methanol immediately, and electrons remain in the particles. The electron spectrum cannot be explained simply by considering the free-electron spectrum. In addition to the broad free-electron band in the background, we also observed a hump with a maximum at around 900 nm. The background spectrum that was fit to λ^n ($n = 1.7$) is shown by the dashed line in Figure 5a. Figure 5b shows the broad spectrum obtained when the dashed line was subtracted from the solid line. The peak at 770 nm was assigned to the absorption band due to electrons other

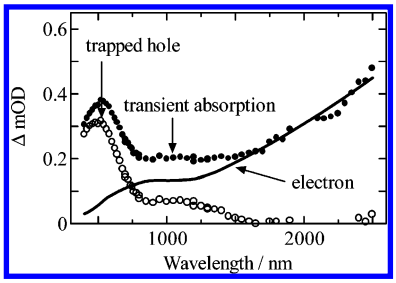

Figure 6. Transient absorption spectrum of a TiO_2 film in N_2-saturated D_2O (●). The solid line (—) represents the absorption spectrum of electrons normalized in the near-IR wavelength range. The open circles (○) represent the subtraction spectrum.

than free electrons. The fact that the spectrum has a peak suggests that the electrons were locally trapped. It is possible that this band is not due to surviving holes. However, the fact that the band intensity decreased in the presence of molecular oxygen (discussed in detail later) removes any doubt.

The absorption spectrum of the holes was obtained by subtracting the electron absorption bands from the transient absorption spectrum in Figure 1. The absorption spectrum of electrons can be reproduced from the spectra of free electrons and trapped electrons. Figure 6 shows the transient absorption spectrum and the reproduced absorption spectrum of electrons normalized in the near-IR wavelength range above 1500 nm. We assigned the subtracted spectrum to the holes. The absorption spectrum of the holes has peaks at 520 and ∼1200 nm. The origin of the absorption peaks is unclear. However, it is notable that the peak position reflects the trap depth of the holes; that is, the holes with the peak at 520 nm were trapped deeper than those with the peak at 1200 nm.

Comparison of the Absorption Spectra of Holes and Electrons with Published Spectra. Because we assigned the peaks in our spectra, we can compare them with literature spectra. Previously reported absorption spectra of holes and electrons in TiO_2 particles are summarized in Figure 7a and b. As already mentioned, the spectra of holes and electrons are sensitive to surface conditions. Thus, a strict comparison of these spectra is difficult, but we can discuss the similarity of peak positions and spectral shapes.

The absorption spectrum of holes with a peak at 450 nm was measured by means of transient absorption spectroscopy in the presence of a electron scavenger, Pt nanoparticles (Figure 7a, H1).[28,29,39] The spectrum of holes has also been obtained by femtosecond spectroscopy.[41] An absorption band with a peak at 520 nm (Figure 7a, H2) was observed in the very early time range. This absorption band becomes broader and shifts toward the shorter-wavelength side.[41] These changes imply that the H2 spectrum is due to unrelaxed (probably shallowly trapped) holes.

We obtained a broad absorption band with peaks at 520 and 1200 nm (Figure 7c, hole). The peak position at 520 nm is similar to the peak positions of H1 and H2. Thus, our assignment is consistent with those of previous work. Ours is the first report of the absorption spectrum of holes in the near-IR wavelength range. Therefore, we cannot compare the absorption band with the peak at 1200 nm with bands observed in other studies.

As we discussed, the absorption spectrum of nanocrystalline films in the near-IR wavelength range can be assigned to the spectrum of free electrons on the basis of similarity with reported spectra.[52,53,58] The spectral shapes, which are determined by the value of n, are similar in each group because free electrons are present in the bulk phase of TiO_2. Thus, the spectral shape is not sensitive to the sample conditions. The absorption spectrum of trapped electrons in the visible wavelength range was obtained

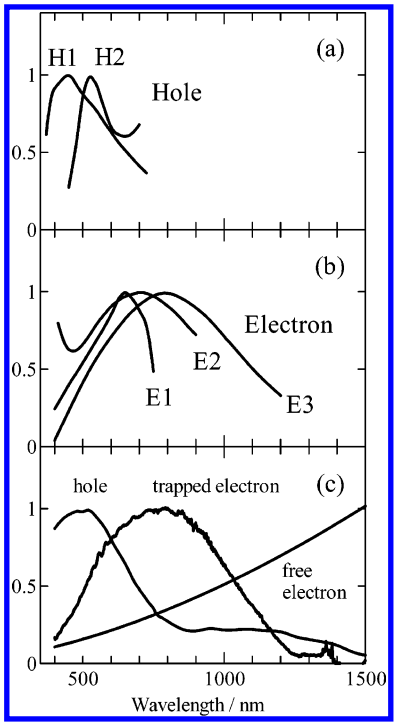

Figure 7. Absorption spectra of trapped holes (a) and trapped electrons (b) found in the literature. The spectra of trapped holes, free electrons, and trapped electrons measured in this work are shown in (c).

through transient absorption measurements in the presence of a hole scavenger such as poly(vinyl alcohol) (Figure 7b, E1).[28,29] The spectrum of the electrons can be also obtained by UV light irradiation in degassed methanol (Figure 7b, E2)[16−18] and in alkaline aqueous solution in the presence of poly(vinyl alcohol) (Figure 7b E3).[31] In the present study, we observed a broad absorption band with a peak at 770 nm in addition to the absorption spectrum due to free electrons. The band position and the spectral shape are similar to those of previously reported spectra. The electron spectrum is very sensitive to the surface conditions. In fact, for nanoparticles in solution, the relative intensity around 770 nm compared with the near-IR range is stronger than that of the nanocrystalline film observed in this work. This result implies that there are many traps for electrons on the particles and that these traps disappear during the preparation of the nanocrystalline film from the particles.

The absorption spectrum of electrons in TiO_2 nanoparticles has also been obtained by an electron pulse radiolysis technique.[19−22,43] This technique allows the production of only electrons in particles. Rabani and co-workers observed changes in the spectral shape of electrons when the nanoparticles were annealed in solution.[22] The relative intensity of the free-electron spectrum compared with that of the trapped electron spectrum becomes pronounced, which suggests that annealing eliminates the traps. Recently, the effect of surface modification by chemical treatment was examined. Dimitrijević et al. observed that absorption due to trapped electrons disappears when the surface is covered with dopamine molecules.[43]

By comparing the published spectra of various samples in various spectral ranges with the present one for an identical sample under different conditions in a wide spectral range (400−2500 nm), we can explain the transient absorption spectrum of TiO_2 particles as follows. There are three transient species: trapped holes, trapped electrons, and free electrons. In the visible wavelength range, all of the spectra overlap. The absorption spectrum of the trapped holes appears at ∼520 nm, and that of the trapped electrons appears at ∼770 nm. The absorption

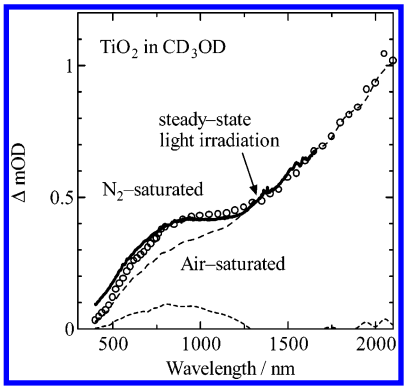

Figure 8. Transient absorption spectra of a TiO_2 film in N_2-saturated CD_3OD (○) and air-saturated CD_3OD (- - -). The dotted line (•• •) represents the subtraction spectrum. The absorption spectrum of electrons obtained from the steady-state irradiation study (Figure 5) is indicated by the solid line (—).

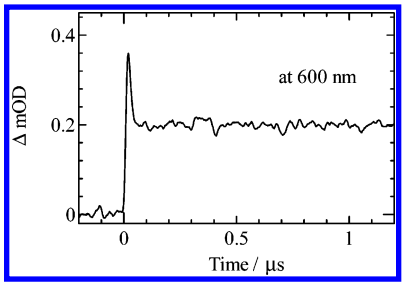

Figure 9. Temporal profiles of transient absorption observed at 600 nm in N_2-saturated CD_3OD.

spectrum of the free electrons appears over a wide wavelength range from visible to infrared. Its intensity increases with increasing wavelength. These facts indicate that transient absorption measurements over a wide wavelength range are essential for following chemical reactions in TiO_2 nanoparticles.

Reaction of a Hole and an Electron in Nanocrystalline TiO_2 Films. Figure 8 shows the transient absorption spectrum of nanocrystalline TiO_2 films in CD_3OD with a delay time of 100 ns. As expected from the steady-state light-irradiation experiment (Figure 5), holes reacted with CD_3OD immediately; therefore, the electrons remained in the film. In fact, the transient absorption spectrum in Figure 8 is identical to that shown in Figure 5a. Figure 9 shows the time profile of the transient absorption signal recorded at 600 nm. In contrast with the decay profile in Figure 3, the decay in Figure 9 is fast (spike), and the subsequent decay is considerably slower. This result clearly shows that holes disappear very rapidly and therefore that electrons can avoid recombination with holes. During the measurements, we did not observe an accumulation of electrons in the film; that is, all of the electrons decayed within the repetition period of the excitation pulsed laser (10 Hz). As shown in Figure 2, the recombination between holes and electrons in the absence of scavengers occurred on the microsecond time scale, which suggests that both holes and electrons move slowly in the particles. Nevertheless, holes are rapidly captured by methanol, within 50 ns, which indicates that holes are localized at or near the surface of the particles.

The dashed line in Figure 8 shows the spectrum in air-saturated CD_3OD solution observed 100 ns after excitation. The absorbance of the trapped electrons clearly decreases, but no change was observed for the free electrons. This result indicates that trapped electrons react with oxygen very rapidly. This suggests that trapped electrons are localized at the surface of the particles. As we mentioned above, free electrons disappear within at least 100 ms, suggesting that free electrons react with

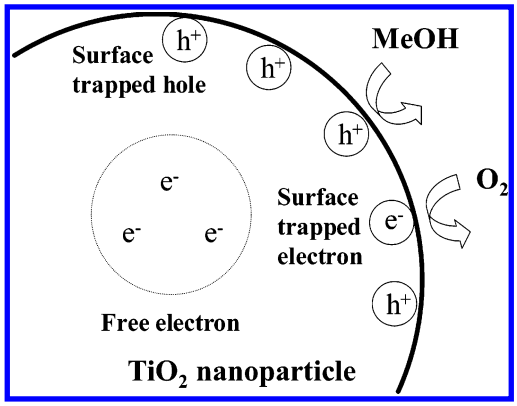

Figure 10. Spatial distribution of holes and electrons in a TiO_2 nanoparticle.

oxygen much more slowly than do trapped electrons. The reaction of free electrons probably occurs stepwise. First, free electrons in the bulk are trapped at the surface-trap site and then react with oxygen immediately. The first step may be the rate-limiting process, and it occurs within microseconds to milliseconds. Transient IR spectroscopy indicates that free electrons react with oxygen molecules on a microsecond time scale.[53] This result is consistent with our observation that the trap site for the electrons at the surface can act as a "gate" for the reaction at the surface.

From the analysis of the transient absorption spectra, we confirmed that trapped holes, trapped electrons, and free electrons were generated upon photoexcitation. The holes and trapped electrons were localized at the surface of the particle, and the free electrons were distributed in the bulk phase. Figure 10 illustrates the spatial distribution of holes and electrons in TiO_2 nanoparticles. This distribution can be explained by conventional solid-state physics; that is, the energy of the conduction band of n-type semiconductors decreases with increasing depth from the surface (band bending) so that electrons are accumulated in the bulk and holes are localized at the surface. Actually, because there are some electron traps at the surface, some electrons are captured at the surface.

Conclusion

We successfully identified the reactive species involved in the very broad transient absorption spectrum of nanocrystalline TiO_2 films. Trapped holes and electrons had absorption peaks at 520 and 770 nm, respectively. The absorbance of free electrons increased with increasing wavelength, and it was strong in the IR range. We believe that the assignment of these species will be useful for studying the mechanisms of reactions on TiO_2 surfaces. We also investigated the reactivity of these species. Trapped holes and electrons reacted with scavenger molecules immediately, whereas free electrons reacted very slowly. On the basis of these facts, we conclude that trap sites are distributed mainly at the surface of particles and free electrons are distributed in the bulk.

Acknowledgment. This work was supported by the COE development program and by a Grant-in-Aid for Scientific Research from the Ministry of Education, Culture, Sports, Science and Technology (MEXT) of Japan.

References and Notes

(1) Fujishima, A.; Honda, K. *Nature* **1972**, *238*, 37−38.
(2) Fujishima, A.; Rao, T. N.; Tryk D. A. *J. Photochem. Photobiol., C* **2000**, *1*, 1−21.
(3) Fujishima, A.; Hashimoto, K.; Watanabe T. *Photocatalysis*; BKC Inc: Tokyo, 1999.
(4) O'Regan, B.; Grätzel, M. *Nature* **1991**, *353*, 737−740.
(5) Nazeeruddin, M. K.; Kay, A.; Rodicio, I.; Humphry-Baker, R.; Muller, E.; Liska, P.; Vlachopoulos, N.; Grätzel, M. *J. Am. Chem. Soc.* **1993**, *115*, 6382−6390.
(6) Hagfeldt, A.; Grätzel, M. *Chem. Rev.* **1995**, *96*, 49−68.
(7) Hoffmann, M. R.; Martin, S. T.; Choi, W.; Bahnemann, D. W. *Chem. Rev.* **1995**, *95*, 69−96.
(8) Kamat, P. V. *Chem. Rev.* **1993**, *93*, 267−300.
(9) Fox, M. A.; Dulay, M. T. *Chem. Rev.* **1993**, *93*, 341−357.
(10) Linsebigler, A. L.; Lu, G.; Yates, J. T., Jr. *Chem. Rev.* **1995**, *95*, 735−758.
(11) Nozik, A. J.; Memming, R. *J. Phys. Chem.* **1996**, *100*, 13061−13078.
(12) Anpo, M.; Takeuchi, M. *J. Catal.* **2003**, *216*, 505−516.
(13) Matsushita, S. I.; Miwa, T.; Tryk, D. A.; Fujishima, A. *Langmuir* **1998**, *14*, 6441−6447.
(14) Sayama, K.; Augustynski, J.; Arakawa, H. *Chem. Lett.* **2002**, 994−995.
(15) Santato, C.; Odziemkowski, M.; Ulmann, M.; Augustynski, J. *J. Am. Chem. Soc.* **2001**, *123*, 10639−10649.
(16) Vinodgopal, K.; Bedija, I.; Hotchandani, S.; Kamat, P. V. *Langmuir* **1994**, *10*, 1767−1771.
(17) Kamat, P. V.; Bedija, I.; Hotchandani, S. *J. Phys. Chem.* **1994**, *98*, 9137−9142.
(18) Jakob, M.; Levanon, H.; Kamat, P. V. *Nano Lett.* **2003**, *3*, 353−358.
(19) Henglein, A. *Ber. Bunsen-Ges. Phys. Chem.* **1982**, *86*, 241−246.
(20) Dimitrijević, N. M.; Savić, D.; Mićić, O. I.; Nozik, A. J. *J. Phys. Chem.* **1984**, *88*, 4278−4283.
(21) Lawless, D.; Serpone, N.; Meisel, D. *J. Phys. Chem.* **1991**, *95*, 5166−5170.
(22) Safrany, A.; Gao, R.; Rabani, J. *J. Phys. Chem. B* **2002**, *104*, 5848−5853.
(23) Howe, R. F.; Grätzel, M. *J. Phys. Chem.* **1985**, *89*, 4495−4499.
(24) O'Regan, B.; Grätzel, M.; Fitzmaurice D. *Chem. Phys. Lett.* **1991**, *183*, 89−93.
(25) Boschloo, G.; Fitmaurice, D. *J. Phys. Chem. B* **1999**, *103*, 2228−2231.
(26) Boschloo, G.; Fitmaurice, D. *J. Phys. Chem. B* **1999**, *103*, 7860−7868.
(27) Duonghong, D.; Ramsden, J.; Grätzel, M. *J. Am. Chem. Soc.* **1982**, *104*, 2977−2985.
(28) Bahnemann, D.; Henglein, A.; Lilie, J.; Spanhel, L. *J. Phys. Chem.* **1984**, *88*, 709−711.
(29) Bahnemann, D.; Henglein, A.; Spanhel, L. *Faraday Discuss. Chem. Soc.* **1984**, *78*, 151−163.
(30) Kirk, A. D.; Langford, C. H.; Joly, C. S.; Lesage, R.; Sharma, D. K. *J. Chem. Soc., Chem. Commun.* **1984**, 961−962.
(31) Kölle, U.; Moser, J.; Grätzel, M. *Inorg. Chem.* **1985**, *24*, 2253−2258.
(32) Rothenberger, G.; Moser, J.; Grätzel, M.; Serpone, N.; Sharma, D. K. *J. Am. Chem. Soc.* **1985**, *107*, 8054−8059.
(33) Arbour, C.; Sharma, D. K.; Langford, C. H. *J. Chem. Soc., Chem. Commun.* **1987**, 917−918.
(34) Arbour, C.; Sharma, D. K.; Langford, C. H. *J. Phys. Chem.* **1990**, *94*, 331−335.
(35) Lepore, G. P.; Langford, C. H.; Víchová, J.; Vlćek, A., Jr. *J. Photochem. Photobiol., A* **1993**, *75*, 67−75.
(36) Colombo, D. P., Jr.; Roussel, K. A.; Saeh, J.; Skinner, D. E.; Cavaleri, J. J.; Bowman, R. M. *Chem. Phys. Lett.* **1995**, *232*, 207−214.
(37) Skinner, D. E.; Colombo, D. P., Jr.; Cavaleri, J. J.; Bowman, R. M. *J. Phys. Chem.* **1995**, *99*, 7853−7856.
(38) Serpone, N.; Lawless, D.; Khairutdinov, R.; Pelizzetti, E. *J. Phys. Chem.* **1995**, *99*, 16655−16661.
(39) Bahnemann, D. W.; Hilgendorff, M.; Memming, R. *J. Phys. Chem. B* **1997**, *101*, 4265−4275.
(40) Rabani, J.; Yamashita, K.; Ushida, K.; Stark, J.; Kira, A. *J Phys. Chem. B* **1998**, *102*, 1689−1695.
(41) Yang, X.; Tamai, N. *Phys. Chem. Phys. Chem.* **2001**, *3*, 3393−3398.
(42) Ramakrishna, G.; Ghosh, H. N. *Langmuir* **2003**, *19*, 505−508.
(43) Dimitrijević, N. M.; Saponjic, Z. V.; Bartels, D. M.; Thurnauer, M. C.; Tiede, D. M.; Rajh, T. *J. Phys. Chem. B* **2003**, *107*, 7368−7375.
(44) Colombo, D. P., Jr.; Bowman, R. M. *J. Phys. Chem.* **1996**, *100*, 18445−18449.
(45) Ohtani, B.; Bowman, R. M.; Colombo, D. P., Jr.; Kaminami, H.; Noguchi, H.; Uosaki, K. *Chem. Lett.* **1998**.
(46) Furube, A.; Asahi, T.; Masuhara, H.; Yamashita, H.; Anpo, M. *Chem. Lett.* **1997**, 735−736.
(47) Asahi, T.; Furube, A.; Masuhara, H. *Chem. Phys. Lett.* **1997**, *275*, 234−238.

(48) Furube, A.; Asahi, T.; Masuhara, H.; Yamashita, H.; Anpo, M. *J. Phys. Chem. B* **1999**, *103*, 3120−3127.
(49) Furube, A.; Asahi, T.; Masuhara, H.; Yamashita, H.; Anpo, M. *Res. Chem. Intermed.* **2001**, *27*, 177−187.
(50) Furube, A.; Asahi, T.; Masuhara, H.; Yamashita, H.; Anpo, M. *Chem. Phys. Lett.* **2001**, *336*, 424−430.
(51) Asbury, J. B.; Hao, E.; Wang, Y.; Ghosh, H. N.; Lian, T. *J. Phys. Chem. B* **2001**, *105*, 4545−4557.
(52) Yamakata, A.; Ishibashi, T.; Onishi, H. *Chem. Phys. Lett.* **2001**, *333*, 271−277.
(53) Yamakata, A.; Ishibashi, T.; Onishi, H. *J. Phys. Chem. B* **2001**, *105*, 7258−7262.
(54) Yamakata, A.; Ishibashi, T.; Onishi, H. *J. Phys. Chem. B* **2002**, *106*, 9122−9125.
(55) Yamakata, A.; Ishibashi, T.; Onishi, H. *J. Photochem. Photobiol., A* **2003**, *160*, 33−36.
(56) Yamakata, A.; Ishibashi, T.; Onishi, H. *Chem. Phys. Lett.* **2003**, *376*, 576−580.
(57) Szczepankiewicz, S. H.; Colussi, A. J.; Hoffmann, M. R. *J. Phys. Chem. B* **2000**, *104*, 9842−9850.
(58) Szczepankiewicz, S. H.; Moss, J. A.; Hoffmann, M. R. *J. Phys. Chem. B* **2002**, *106*, 2922−2927.
(59) Szczepankiewicz, S. H.; Moss, J. A.; Hoffmann, M. R. *J. Phys. Chem. B* **2002**, *106*, 7654−7658.
(60) Nakamura, R.; Imanishi, A.; Murakoshi, K.; Nakato, Y. *J. Am. Chem. Soc.* **2003**, *125*, 7443−7450.
(61) Barbé, C. J.; Arendse, F.; Comte, P.; Jirousek, M.; Lenzmann, F.; Shklover, V.; Grätzel, M. *J. Am. Ceram. Soc.* **1997**, *80*, 3157−3171.
(62) Hara, K.; Horiguchi, T.; Kinoshita, T.; Sayama, K.; Sugihara, H.; Arakawa, H. *Sol. Energy Mater. Sol. Cells* **2000**, *64*, 115−134.
(63) Haque, S. A.; Tachibana, Y.; Willis, R. L.; Moser, J. E.; Grätzel, M.; Klug, D. R.; Durrant, J. R. *J. Phys. Chem. B* **2000**, *104*, 538−547.
(64) Barzykin, A. V.; Tachiya, M. *J. Phys. Chem. B* **2002,** *106*, 4356−4363.
(65) Clifford, J. N.; Yahioglu, G.; Milgrom, L. R.; Durrant, J. R. *Chem. Commun.* **2002**, 1260−1261.
(66) Tamaki, Y.; Furube, A.; Katoh, R.; Yoshihara T.; Hara, K.; Murai, M.; Murata, S.; Arakawa, H.; Tachiya, M. To be submitted for publication.
(67) Pankove, J. I. *Optical Processes in Semiconductors*; Dover: New York, 1975.
(68) Katoh, R.; Furube, A.; Hara, K.; Murata, S.; Sugihara, H.; Arakawa, H.; Tachiya, M. *J. Phys. Chem. B* **2002,** *106*, 12957−12964.
(69) Furube, A.; Katoh, R.; Hara, K.; Murata, S.; Arakawa, H.; Tachiya, M. *J. Phys Chem B* **2003**, *107*, 4162−4166.